Langmuir
Article
pubs.acs.org/Langmuir

Correlating Linactant Efficiency and Self-Assembly: Structural Basis of Line Activity in Molecular Monolayers

Siwar Trabelsi,[†] Zhongcheng Zhang,[‡] Shishan Zhang,[‡] T. Randall Lee,[‡] and Daniel K. Schwartz*,[†]

[†]*Department of Chemical and Biological Engineering, University of Colorado, Boulder, Colorado 80309-0424, and* [‡]*Department of Chemistry, University of Houston, Houston, Texas 77204-5003*

Received February 15, 2009. Revised Manuscript Received March 29, 2009

Surfactants exhibit characteristic phenomena, including the reduction of interfacial free energy, self-assembly into aggregates, and even the formation of lyotropic liquid crystalline phases at high concentrations. Our research has shown that a semifluorinated phosphonic acid can act as the two-dimensional analogue of a surfactant-a linactant-by reducing the line tension between hydrocarbon-rich and fluorocarbon-rich phases in a Langmuir monolayer. This linactant can also self-assemble into nanoscale clusters in a monolayer. Here, we explore the dependence of linactant behavior on molecular structure. Members of a homologous series of partially fluorinated phosphonic acids were synthesized and tested as linactants: $CF_3(CF_2)_{n-1}(CH_2)_mPO_3H$ (abbreviated as **FnHmPO$_3$**). The tests revealed that linactants with longer hydrophobic chains were most efficient in lowering line tension. For linactants with the same overall chain length, the length of the fluorocarbon block was correlated with efficiency. Thus, the linactant efficiency was ranked in the order **F8H8PO$_3$** < **F10H6PO$_3$** < **F8H11PO$_3$** < **F10H9PO$_3$**. In all cases, linactant-containing Langmuir−Blodgett monolayers exhibited nanoscale molecular clusters with characteristic dimensions of 20−30 nm; enhanced linactant efficiency was systematically correlated with larger clusters.

Introduction

The performance of surfactant molecules in lowering the interfacial tension of a solution is classically characterized by two macroscopic properties: efficiency and effectiveness.[1] The surfactant efficiency is related to the change in bulk surfactant concentration necessary to reduce the surface tension by a given amount. Effectiveness, on the other hand, refers to the maximum reduction in surface tension that can be obtained by the addition of a given surfactant. Surfactant efficiency is strongly influenced by the length of the hydrophobic chain; typically, the longer the hydrophobic chain, the more efficient the surfactant.[1] Fluorinated surfactants have been shown to exhibit high efficiency in reducing surface tension[2,3] due to relatively low cohesive energy density and associated weak intermolecular interactions. The effectiveness of a surfactant is related to the value of the surface tension at the critical aggregate concentration (cac), which is the concentration at which surfactant molecules self-assemble into well-defined structures such as micelles or bilayers. Increasing the surfactant concentration beyond the cac typically leads to only a small additional reduction in the surface tension.

By analogy to surfactants in three-dimensional (3D) systems, a new class of molecules that we call "linactants" plays a surfactant-like role in Langmuir monolayers-monolayers of insoluble surfactant at the air/water interface. Linactants can be used to stabilize coexisting nano- and mesoscale two-dimensional (2D) domains within a monolayer by reducing the line tension.[4] There has been a recent renewed interest in immiscibility and inhomogeneity within monolayers and bilayers for several reasons, including the development of patterned biomimetic bilayers for sensor applications, and recent discoveries related to phase separation in pulmonary surfactant layers[5−9] and "lipid rafts" within biological membranes.[10,11] Rafts are submicron domains that are enriched in cholesterol and sphingolipids; they have a demonstrated role in cell signaling. It has been proposed that rafts are formed due to the differential miscibility of various lipids within bilayer membranes.[12−14] The putative size of lipid rafts is in the 40−100 nm range, making the reduction of line tension a requirement for raft stability.

We[15,16] and others[17−21] have also observed linactants and similar partially fluorinated compounds to form self-organized molecular nanostructures at high surface concentrations. In typical 3D surfactant self-assembly, aggregates are formed having

*To whom correspondence should be addressed: E-mail: Daniel.Schwartz@colorado.edu, phone 303-735-0240, fax 303-492-4341.

(1) Myers, D. Surfaces, Interfaces, and Colloids. Principles and Applications. In *Surfaces, Interfaces, and Colloids. Principles and Applications*, 2nd ed.; Wiley-VCH: Weinheim, 1999.
(2) Yoshimura, T.; Ohno, A.; Esumi, K. *Langmuir* **2006**, *22* (10), 4643−4648.
(3) Riess, J. G. *Tetrahedron* **2002**, *58* (20), 4113−4131.
(4) Trabelsi, S.; Zhang, S.; Lee, T. R.; Schwartz, D. K. *Phys. Rev. Lett.* **2008**, *100* (3), 037802.
(5) Bringezu, F.; Ding, J. Q.; Brezesinski, G.; Zasadzinski, J. A. *Langmuir* **2001**, *17* (15), 4641−4648.
(6) Ding, J. Q.; Doudevski, I.; Warriner, H. E.; Alig, T.; Zasadzinski, J. A. *Langmuir* **2003**, *19* (5), 1539−1550.
(7) Discher, B. M.; Maloney, K. M.; Grainger, D. W.; Hall, S. B. *Biophys. Chem.* **2002**, *101*, 333−345.
(8) Gopal, A.; Lee, K. Y. C. *J. Phys. Chem. B* **2001**, *105* (42), 10348−10354.
(9) Takamoto, D. Y.; Lipp, M. M.; von Nahmen, A.; Lee, K. Y. C.; Waring, A. J.; Zasadzinski, J. A. *Biophys. J.* **2001**, *81* (1), 153−169.
(10) Brown, D. A. *Proc. Natl. Acad. Sci. U.S.A.* **2001**, *98* (19), 10517−10518.
(11) Lipowsky, R. *J. Biol. Phys.* **2002**, *28* (2), 195−210.
(12) Rietveld, A.; Simons, K. *Biochim. Biophys. Acta* **1998**, *1376* (3), 467−479.
(13) Hermelink, A.; Brezesinski, G. *J. Lipid Res.* **2008**, *49* (9), 1918−1925.
(14) Honerkamp-Smith, A. R.; Cicuta, P.; Collins, M. D.; Veatch, S. L.; den Nijs, M.; Schick, M.; Keller, S. L. *Biophys. J.* **2008**, *95* (1), 236−246.
(15) Trabelsi, S.; Zhang, S.; Lee, T. R.; Schwartz, D. K. *Soft Matter* **2007**, *3* (12), 1518−1524.
(16) Trabelsi, S.; Zhang, S.; Zhang, Z.; Lee, T. R.; Schwartz, D. K. *Soft Matter* **2009**, *5*, 750−758.
(17) Kato, T.; Kameyama, M.; Ehara, M.; Iimura, K. *Langmuir* **1998**, *14* (7), 1786−1798.
(18) Mourran, A.; Tartsch, B.; Gallyamov, M.; Magonov, S.; Lambreva, D.; Ostrovskii, B. I.; Dolbnya, I. P.; de Jeu, W. H.; Moeller, M. *Langmuir* **2005**, *21* (6), 2308−2316.
(19) Krafft, M. P.; Goldmann, M. *Curr. Opin. Colloid Interface Sci.* **2003**, *8* (3), 243−250.
(20) Maaloum, M.; Muller, P.; Krafft, M. P. *Angew. Chem., Int. Ed.* **2002**, *41* (22), 4331−4334.
(21) Maaloum, M.; Muller, P.; Krafft, M. P. *Langmuir* **2004**, *20* (6), 2261−2264.

at least one characteristic dimension that is related to twice the molecular length (e.g., micelle diameter or bilayer thickness). This dimension corresponds to the head−tail:tail−head arrangement that is common in surfactant aggregates and is consistent with hydrophobic interactions. The lateral size of linactant nanostructures in monolayers, however, was found to be 20−30 nm,[15,16] which is roughly 50 times larger than the cross-sectional diameter of the linactant molecule and at least 10 times the molecular length. The molecular-level basis for these 2D aggregates is not fully understood; however, we have proposed that these dome-shaped structures are caused by the mismatch of close-packing preferences of the hydrocarbon block and the bulkier fluorocarbon block,[16] which gives rise to a subtle splay of the molecular axis in close-packed aggregates.

In our previous work,[4] two partially fluorinated linactant molecules (with one and two tails, respectively) were synthesized, and their line activity was tested with respect to the two-dimensional coexisting phases in a mixed monolayer composed of pentadecanoic acid (**H14**) and perfluoroundecanoic acid (**F10**). The line tension between hydrocarbon-rich and fluorocarbon-rich phases was measured by monitoring the relaxation kinetics of bola-deformed domains back to their equilibrium circular shape.[22−28] We reported that the addition of a small amount of either linactant significantly reduced the line tension between the coexisting 2D phases. Notably, the single-tail linactant (**F8H11PO$_3$**) was dramatically more efficient than the double-tail linactant. These results motivated us to investigate further the structural basis of linactant efficiency by examining a homologous series of single-tail semifluorinated phosphonic acids and to use this system to establish the relationship(s) between linactant self-organization and efficiency.

Materials and Methods

The molecular structures of the semifluorinated phosphonic acid linactants are shown in Figure 1. The synthesis of **F8H11PO$_3$** was described previously.[15] The other semifluorinated linactants (**F8H8PO$_3$**, **F10H6PO$_3$**, and **F10H9PO$_3$**) were prepared using analogous strategies and methods. Pentadecanoic acid (**H14**; Acros Organics) and perfluoroundecanoic acid (**F10**; Oakwood Products Inc.) were dissolved in choloroform (Fisher Scientific). All partially fluorinated phosphonic acid linactants were dissolved in tetrahydrofuran (Fisher Scientific).

Mixed Langmuir monolayers were spread dropwise using a microliter syringe at the air−water interface of a custom-built Langmuir trough. The pH of the subphase was adjusted to 3 by addition of hydrochloric acid (Mallinckrodt). After spreading, the monolayers were allowed to relax for at least 10 min to ensure solvent evaporation. The monolayer was compressed by a motorized barrier at a constant rate of 20 mm/min. The monolayer structure at the air−water interface was visualized using a custom-built Brewster angle microscope (BAM).[29,30] Domain deformation was achieved by shearing the interfacial layer, which was

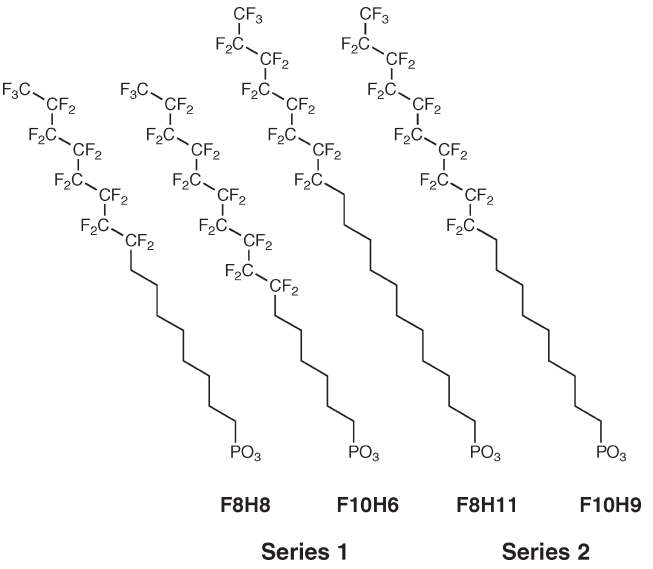

Figure 1. Structures of the semifluorinated phosphonic acid linactants.

performed manually using a syringe needle. The interfacial shear was sufficient to create some domains exhibiting a bola shape, consisting of two disks of radius R connected by a thin string. The BAM was mounted on a joystick-controlled motorized XY translation stage, allowing us to track the bola-shaped domains and to follow the entire relaxation process of individual domains. The bola domains relaxed primarily by a gradual shortening of the string (at constant velocity V) connecting the two disks. Videos of domain relaxation were analyzed frame-by-frame to determine the domain relaxation velocity. The line tension, λ, of a given mixture was determined from measurements of domain recovery kinetics as a function of bola disk radius, R, according to the formula $V = 3\lambda/8\eta R$, where η is the subphase viscosity.[22] In particular, the best value of λ and the uncertainty in λ were determined from linear fits to data where V was plotted versus R^{-1}. This process was repeated for each monolayer composition. Further details of this approach were described previously.[4]

LB monolayers were transferred to freshly cleaved mica substrates by vertical dipping (on the upstroke) at a surface pressure of 4 mN/m. These samples were imaged with a Nanoscope MMAFM (Digital Instruments-now Veeco). Images were obtained in tapping mode using silicon nitride tips at room temperature (23 ± 1 °C) under ambient atmospheric conditions. The size and the height of clusters were measured by analyzing cross-sectional height profiles from AFM images; for close-packed clusters, the characteristic cluster size was taken as the distance between minima in the cross-section profile.

Results

Line Tension Isotherms. It is convenient to divide the linactants into two series based on total chain length: series 1 (**F8H8PO$_3$** and **F10H6PO$_3$**) and series 2 (**F8H11PO$_3$** and **F10H9PO$_3$**). Within each series, the total chain length is fixed while the relative lengths of the hydrocarbon and fluorocarbon blocks vary (see Figure 1).

In the absence of shear, BAM images of two-component **H14**/**F10** monolayers exhibited circular domains of **H14**-rich phase surrounded by a matrix of **F10**-rich phase as shown in Figure 2a. Monolayers containing linactant were qualitatively similar, but with systematically smaller domain sizes, as shown in Figure 2b. In the absence of linactant, the domain size (and average domain coverage) was dramatically heterogeneous over macroscopic length scales, to the extent that it was not practical to measure the domain size distribution. As described above, following the

(22) Benvegnu, D. J.; McConnell, H. M. *J. Phys. Chem.* **1992**, *96* (16), 6820−6824.
(23) Lauger, J.; Robertson, C. R.; Frank, C. W.; Fuller, G. G. *Langmuir* **1996**, *12* (23), 5630−5635.
(24) Mann, E. K.; Henon, S.; Langevin, D.; Meunier, J.; Leger, L. *Phys. Rev. E* **1995**, *51* (6), 5708−5720.
(25) Riviere, S.; Henon, S.; Meunier, J. *Phys. Rev. Lett.* **1995**, *75* (13), 2506−2509.
(26) Roberts, M. J.; Teer, E. J.; Duran, R. S. *J. Phys. Chem. B* **1997**, *101* (5), 699−701.
(27) Steffen, P.; Wurlitzer, S.; Fischer, T. M. *J. Phys. Chem. A* **2001**, *105* (36), 8281−8283.
(28) Wurlitzer, S.; Steffen, P.; Fischer, T. M. *J. Chem. Phys.* **2000**, *112* (13), 5915−5918.
(29) Henon, S.; Meunier, J. *Rev. Sci. Instrum.* **1991**, *62* (4), 936−939.
(30) Honig, D.; Mobius, D. *J. Phys. Chem.* **1991**, *95* (12), 4590−4592.

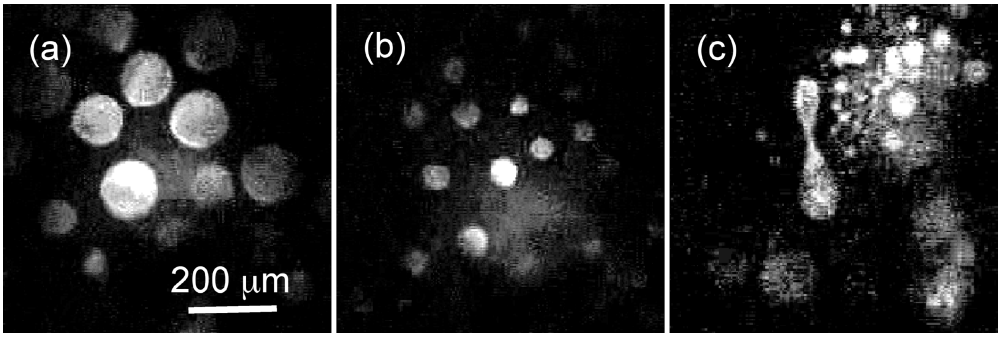

Figure 2. BAM images of two- and three-component monolayers. (a) Two-component monolayer composed of **H14** (96.5%) and **F10** (3.5%) at $\pi = 6$ mN/m. (b) Three-component monolayer (at $\pi = 6$ mN/m) with the same **H14**/**F10** ratio as in (a) but with the addition of 2×10^{-4} mole fraction of **F10H9PO$_3$** linactant. (c) The same composition as in (b) but after the application of interfacial shear.

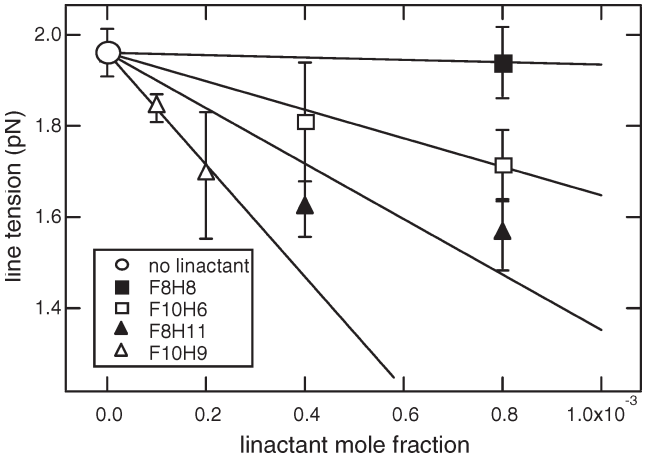

Figure 3. Measured line tension as a function of linactant concentration for a monolayer composed of **H14** (96.5%) and **F10** (3.5%) at $\pi = 6$ mN/m and for monolayers with the same **H14**:**F10** ratio with small amounts of additional linactant.

application of interfacial shear, some of the domains were deformed into unstable bola shapes as shown in Figure 2c.

We previously[4] measured the bare line tension of the two-component **H14**/**F10** mixture to be $\lambda = 1.96 \pm 0.05$ pN. Figure 3 shows the measured values of the modified line tension in the presence of various linactants as a function of the linactant mole fraction within the three-component mixed monolayer. We found that the line tension decreased systematically as the linactant concentration was increased. In general, we were unable to determine the line tension below values of ~1.55 pN. For lower values of line tension, a domain-shaped instability preceded the formation of peanut-shaped instabilities or curved domains,[31] and we were unable to create bola-shaped domains in these monolayers. In particular, this behavior meant that we were unable to extend measurements of the **F10H9PO$_3$** linactant beyond a mole fraction of 2×10^{-4}.

The slopes ($\partial\lambda/\partial C$) of the line tension versus linactant concentration curves (i.e., the linactant efficiencies) are summarized in Table 1. These values show that most of the linactants investigated tended to reduce the line tension, although the efficiency of **F8H8PO$_3$** was essentially negligible. In series 1, we found that the linactant with the longer fluorinated block (**F10H6PO$_3$**) was significantly more efficient than **F8H8PO$_3$**. The same trend was observed for series 2, where the linactant with the longer fluorinated block (**F10H9PO$_3$**) induced a significantly larger decrease of the line tension. Notably, the linactants

Table 1. Linactant Efficiencies and Self-Assembled Cluster Sizes

	linactant	$-(\partial\lambda/\partial X)$ (10^{-10} N)	cluster size (nm)
series 1	**F8H8PO$_3$**	0.3 ± 1	19 ± 2
	F10H6PO$_3$	3 ± 1	21 ± 1
series 2	**F8H11PO$_3$**	6 ± 1	28 ± 2
	F10H9PO$_3$	13 ± 5	34 ± 1

of series 2 were more efficient than those of series 1. These results suggest that the overall chain length and the length of the fluorocarbon block are both factors that enhance linactant efficiency. Interestingly, the relatively subtle changes in molecular architecture gave rise to significant changes in linactant activity. In fact, the linactant efficiency varied by more than an order of magnitude within these four compounds. Notably, 3D surfactant efficiency is also generally enhanced by increased chain length or the presence of fluorocarbon moieties.

For 3D surfactant solutions, measurements of surface tension isotherms permit a calculation of the surface excess surfactant concentration using the Gibbs equation. An analogous expression can be derived in 2D to calculate the line excess concentration of linactant. At the low linactant concentrations used in the line tension experiments reported here (i.e., well below the critical concentration for 2D aggregate formation), the linactant activity is approximately proportional to the linactant concentration, and an appropriate expression is

$$\Gamma = -\frac{1}{RT}\left(\frac{\partial\lambda}{\partial \ln C}\right)_{T,\pi} = -\frac{C}{RT}\left(\frac{\partial\lambda}{\partial C}\right)_{T,\pi}$$

where Γ is the line excess concentration, R is the gas constant, T is the absolute temperature, C is the linactant concentration, and λ is the line tension. Assuming that all isotherms are approximately linear in the dilute regime shown in Figure 3, these calculations gave small values of the line excess concentration that were < 0.1 molecule/nm, which is approximately an order of magnitude smaller than one would expect for a close-packed layer of linactant at the phase boundary. This result suggests that our method of measuring the line tension is limited, by the occurrence of the domain-shaped instability, to the initial Henry's law region of the adsorption isotherm.

Domain Boundary Structure. In our previous work,[4] AFM images of the two-component **H14**/**F10** monolayer showed that the boundaries between the hydrocarbon-rich and fluorocarbon-rich areas were well-defined and relatively smooth. When a small amount of **F8H11PO$_3$** was added, the boundaries became rough and highly ramified, with fingers extending into the surrounding phase. Similar structures were observed with all of the linactants investigated here. As a representative example, Figure 4 shows AFM images of domain edges in the **H14**/**F10** binary system and

(31) McConnell, H. M.; Moy, V. T. *J. Phys. Chem.* **1988**, *92* (15), 4520−4525.

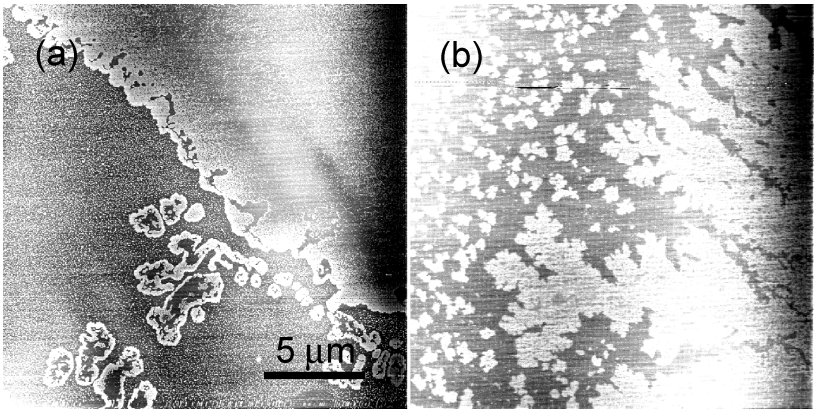

Figure 4. AFM images of Langmuir−Blodgett monolayers transferred at 4 mN/m. (a) Two-component monolayer composed of **H14** (96.5%) and **F10** (3.5%). (b) Three-component monolayer with the same **H14**/**F10** ratio as in (a) but with the addition of 2×10^{-4} mole fraction of **F10H9PO$_3$** linactant.

the **H14**/**F10**/**F10H9PO$_3$** system. The qualitative difference in the nanoscale appearance of the domain edges provides further support for our hypothesis that the linactant partitions to the domain boundaries. However, we believe that it is likely that the specific structure of the boundaries may form during the LB deposition process. For example, the domain shown in Figure 4b exhibits roughness on length scales of several micrometers, which should be visible using BAM; however, we see no evidence of rough boundaries in BAM images at the air/water interface. Previous work in our group has suggested that long-range interactions of the monolayer with the solid substrate during LB deposition can cause fingering instabilities[32,33] under appropriate conditions. The key point here is that there is a qualitative difference in the boundary morphology of the deposited domains with or without very small quantities of added linactant.

Linactant Self-Assembly in Two-Dimensions. To establish a relation between the linactant efficiency and self-organization, single-component monolayers of the various linactants were transferred by Langmuir−Blodgett (LB) method to mica substrates and analyzed using AFM. As previously reported for monolayers of related semifluorinated phosphonic acids,[15] as well as for monolayers of other semifluorinated compounds,[17−21] the AFM images showed the presence of 2D molecular clusters with characteristic sizes of 19−34 nm (see Figure 5). Since these monolayers were composed of pure linactant, the appropriate analogy with 3D surfactant systems would be to lyotropic liquid crystal phases at very high concentrations. Like typical lyotropic phases, many of the LB monolayers exhibited long-range liquid crystalline order with respect to the arrangement of clusters.

Table 1 summarizes the size of the clusters measured using a cross-sectional analysis. The apparent height of the clusters, for all linactants, was significantly smaller than the extended molecular lengths, suggesting that the molecules were not fully extended, that the low areas did not correspond to bare substrate, and/or that the clusters were so closely crowded that the AFM tip was not able to probe fully the lower regions separating them.

Table 1 shows that the characteristic lateral dimension of the clusters increases significantly with total chain length (series 1 vs series 2); a less dramatic increase in cluster size is observed with increasing fluorocarbon block length within a given series. Notably, this same trend was observed for linactant efficiency. Indeed, Table 1 shows a systematic correlation between the measured linactant efficiency (in a three-component monolayer) and the observed cluster size (in a one-component monolayer). Although these observations are empirical, they establish an interesting correlation between the macroscopic properties of the linactant compounds (associated with line-tension modification) and the nanometer-scale properties associated with molecular packing. The correlation might be due to the fact that both properties are related to the internal chemical incompatibility of the molecules associated with covalently linked hydrocarbon and fluorocarbon blocks.

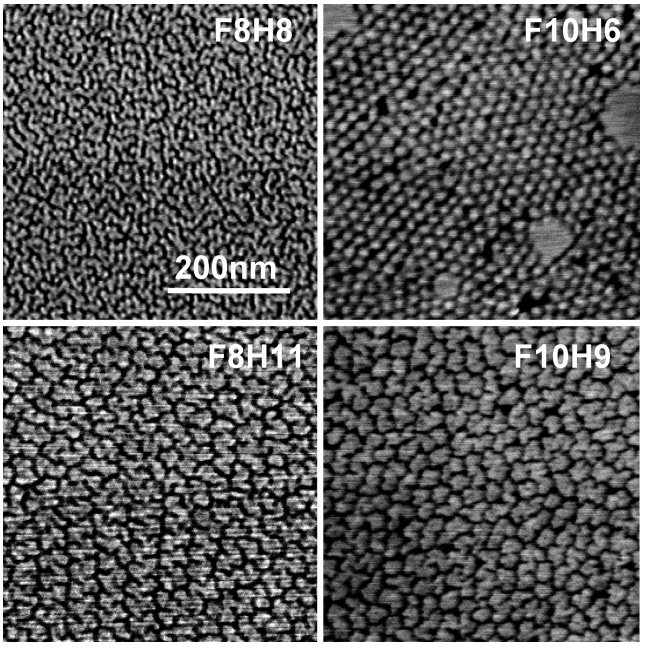

Figure 5. AFM images of one-component linactant LB monolayers composed of semifluorinated phosphonic acids (the particular linactant compounds are indicated by the annotation of the images). The monolayers were transferred onto mica at 4 mN/m.

Discussion

Semifluorinated linactants exhibit phenomena, both macroscopic and microscopic, in 2D that are analogous to those of surfactants in 3D solutions. In three-component monolayers, the linactants reduce the line tension associated with boundaries between hydrocarbon-rich and fluorocarbon-rich monolayer phases. The degree of line tension reduction increases with linactant concentration, and the efficiency of the reduction increases with hydrophobic chain length. All of these effects are

(32) Sikes, H. D.; Schwartz, D. K. *Langmuir* **1997**, *13* (17), 4704−4709.
(33) Sikes, H. D.; Woodward, J. T.; Schwartz, D. K. *J. Phys. Chem.* **1996**, *100* (21), 9093−9097.

Figure 6. Proposed packing of semifluorinated phosphonic acid linactants in one-component monolayers.

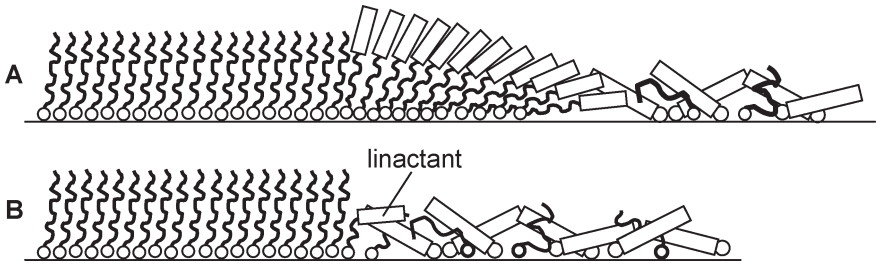

Figure 7. Proposed arrangement of linactants at the boundary between a hydrocarbon-rich and fluorocarbon-rich monolayer phase. (a) Hypothetical linactant arrangement under the conditions of concentrated boundary adsorption. (b) Dilute linactant adsorption consistent with the isotherms reported here.

directly analogous to the effects that typical surfactants have on interfacial tension (e.g., in oil/water systems). Furthermore, the presence of linactants led to a reduction in the size of discrete micrometer-scale hydrocarbon-rich domains. In the absence of linactants, these domains often coalesced into macroscopic regions. These observations are reminiscent of the stabilizing effects that surfactants exert upon oil/water emulsions. The mechanism by which this stabilization occurs in 3D systems involves the reduction of droplet coalescence rates due to the Gibbs−Marangoni effect. We have yet to develop a mechanistic understanding of how linactants stabilize the observed 2D fluorocarbon/hydrocarbon "emulsions".

At nanometer-length scales, linactants are observed to form well-defined aggregates in neat one-component monolayers; in some cases, these aggregates exhibit long-range liquid crystalline order. This behavior appears to be analogous to the formation and lateral organization (into lyotropic liquid crystal phases) of micelles or other aggregates in concentrated surfactant solutions. However, in contrast with 3D aggregates, whose characteristic dimension is typically twice the molecular length, the 2D aggregates are significant larger in their lateral dimensions. This phenomenon suggests that the specific molecular mechanisms leading to aggregation are likely to be somewhat different. We previously proposed[15,16] that the formation of finite-sized clusters in these systems could be due to the incompatibility between the close-packing requirements of the hydrocarbon (nearest-neighbor distance of 0.48 nm)[34] and fluorocarbon (nearest-neighbor distance of 0.585 nm)[35] blocks. Packing frustration due to incompatible blocks has been shown to lead to transitions between surface phases in melts of semifluorinated alkanes.[36] One strategy to compensate for this incompatibility, while preserving both hydrocarbon−hydrocarbon and fluorocarbon−fluorocarbon interactions to some degree, involves packing the slightly wedge-shaped molecules in a splayed configuration. This arrangement leads to spontaneous curvature as shown in Figure 6. A related structure was considered by Moeller and co-workers[18] for the unidirectional "ribbons" that they observed in thin films of partially fluorinated alkanes.

The approximate angle associated with such a molecular wedge can be estimated with the formula $\Delta\theta = \Delta d/l$, where Δd refers to the difference between the fluorocarbon and hydrocarbon nearest-neighbor distances and l is the molecular length. This approximation gives a value of $\Delta\theta \approx (0.1\text{ nm})/(2\text{ nm}) = 0.05$. Close packing of such wedges standing on a flat surface would lead to frustration when the accumulated angle reached π, which would require approximately $\pi/\Delta\theta = 62$ molecules. Given the nearest-neighbor distance of ~0.5 nm, such a cluster would be roughly 30 nm in diameter, which is similar to what we observe. The domelike shapes of the **F8H8PO$_3$** clusters observed previously with AFM are consistent with this picture.[16] While we readily admit that this model is oversimplified, and one cannot expect quantitative agreement between predicted and measured length scales, it is nevertheless interesting to consider the trends that such a model would predict. Given that the wedge angle is inversely proportional to total chain length, this model suggests that longer molecules would give rise to larger clusters, which is qualitatively consistent with our observations in Table 1. It is also intuitive that for two molecules with the same overall chain length the molecule with a longer fluorocarbon block would have a larger wedge angle, although to make this prediction quantitative would require a more refined estimate of the wedge angle.

Gallyamov and co-workers[37] derived a related geometric model to describe the lateral size of toroidal structures formed by partially fluorinated alkanes. Their simplified formula did not account explicitly for the effect of the fluorocarbon block length and predicted that the aggregate diameter depended mainly on the length of the hydrocarbon block. While this prediction is not quite in agreement with our observations, we note that their formula gives aggregate diameters that are within ~30% of our measured values.

How might linactant molecules be arranged at the boundary between hydrocarbon-rich and fluorocarbon-rich monolayer phases? If one accepts that the linactant molecules have a tendency to pack in a slightly splayed arrangement, one can imagine a partial cluster structure at the boundary that would maximize molecular interactions. Such a structure is illustrated in Figure 7a. This structure, however, has a large excess of linactant molecules at the boundary, which, although possible, is not consistent with the situation under the conditions of our experiments, where the boundary adsorption is quite weak. A speculative arrangement consistent with a small boundary excess of linactant is illustrated in Figure 7b.

(34) Barton, S. W.; Thomas, B. N.; Flom, E. B.; Rice, S. A.; Lin, B.; Peng, J. B.; Ketterson, J. B.; Dutta, P. *J. Chem. Phys.* **1988**, *89* (4), 2257−2270.
(35) Barton, S. W.; Goudot, A.; Bouloussa, O.; Rondelez, F.; Lin, B. H.; Novak, F.; Acero, A.; Rice, S. A. *J. Chem. Phys.* **1992**, *96* (2), 1343−1351.
(36) Gang, O.; Ellmann, J.; Moller, M.; Kraack, H.; Sirota, E. B.; Ocko, B. M.; Deutsch, M. *Europhys. Lett.* **2000**, *49* (6), 761−767.
(37) Gallyamov, M. O.; Mourran, A.; Tartsch, B.; Vinokur, R. A.; Nikitin, L. N.; Khokhlov, A. R.; Schaumburg, K.; Moeller, M. *Phys. Chem. Chem. Phys.* **2006**, *8*, 2642−2649.

Conclusions

The various linactants investigated in this paper (**F8H8PO$_3$**, **F10H6PO$_3$**, **F8H11PO$_3$**, and **F10H9PO$_3$**) reduce the line tension in three-component monolayers and also self-assemble into nanometer-scale aggregates in one-component monolayers. Our results suggest a molecular design strategy for linactants that incorporates three distinct moieties: an anchoring headgroup and a dual-component tail consisting of two different segments, each of which is compatible with one of the coexisting phases (fluorocarbon and hydrocarbon in our case). We hypothesize that the incompatibility of close-packing requirements for the hydrocarbon and fluorocarbon segments causes frustration in the long-range order within one-component linactant monolayers, leading to the finite-sized aggregates or even periodic structures in some cases. This behavior might be a general feature of linactant monolayers. Both linactant efficiency and the details of the self-assembly are closely correlated to the molecular structure of the linactant molecule. In particular, linactants with longer hydrophobic chains are more efficient, and for a given total chain length, linactants with longer fluorocarbon blocks are more efficient. These same molecular properties dictate the characteristic length scale of the self-assembled aggregates, offering a direct correlation between linactant efficiency and aggregate size.

Acknowledgment. This research was supported by NSF awards DMR-0447585 (S.T. and D.K.S.) and DMR-0447588 (Z.Z., S.Z., and T.R.L.).